ROCKY MOUNTAIN
JOURNAL OF MATHEMATICS
Volume 41, Number 3, 2011

FORMATION CONTROL OF A SWARM OF MOBILE MANIPULATORS

BIBHYA SHARMA, JITO VANUALAILAI AND AVINESH PRASAD

ABSTRACT. This paper presents a new Lyapunov-based decentralized formation control planner for a swarm of 2-link mobile manipulators in an *a priori* known environment. To ensure a significant degree of formation stiffness along the flight-path, information on moving ghost targets, inter-robot bounds for aggregation and heading for the mobile manipulators are captured in the control planner. The final desired orientation of the formation is by observing a minimum distance between every member of the swarm and ghost walls. The nonlinear control laws extracted from the Lyapunov-based control scheme are utilized to obtain collision-free trajectories of the swarm in a low-degree formation, whilst ensuring stability of the kinodynamic system governing the swarm. The effectiveness of the controllers is demonstrated by simulating interesting situations.

1. Introduction. Social interactions in nature have inspired researchers to design numerous robotic systems that are capable of solving real-world problems for humans. One such biological behavior is swarming, a cooperative behavior seen, for example, in schools of fishes, flocks of birds, and herds of animals, to name but a few. This salient behavior is predominantly based on the principle that there is safety and strength in numbers [**5, 17**]. This swarm-intelligence system, if emulated appropriately, can satisfy stringent time, manpower and monetary demands, enhance performances and robustness, and harness desired multi-behaviors, each of which is extremely difficult if not entirely impossible to solicit from single agents [**6, 8, 16, 17**]. These multi-agent formations are tipped to play a very crucial role in the future. In fact, multi-robot formations are frequently sighted in places such as airports, factories, wharfs, and in farms and mines.

2010 AMS *Mathematics subject classification.* Primary 34A30, 34D20, 70E60, 93C85, 93D15.

Keywords and phrases. Mobile manipulators, kinodynamic constraints, low-degree formation, Lyapunov-based control scheme, minimum distance technique, ghost walls, ghost targets.

Received by the editors on February 5, 2008, and in revised form on September 29, 2008.

DOI:10.1216/RMJ-2011-41-3-909

In literature, swarm-intelligence systems consist of three basic rules of steering, namely *separation, alignment* and *cohesion*, which describe how an individual maneuvers based on the positions and velocities of its neighbors [**18**]. Although the rules governing each agent of a group are seemingly basic, the collective motion is strikingly spectacular. The superposition of these three rules results in all agents moving in a particular formation, with a common heading whilst avoiding all possible collisions [**27**].

Control and motion planning of swarm formations have been facilitated via a number of techniques. The much fancied artificial potential fields (APFs) are still highly favored [**1, 7, 11, 12, 13**] appearing frequently in literature. This is mostly due to easier analytic representation of system singularities and inequalities, simplicity and elegance [**23**], favorable processing speeds, decentralization and scalability features [**13**]. The governing principle behind the APFs is to attach attractive field to the target and a repulsive field to each of the obstacles. The whole workspace is then inundated with positive and negative fields, with the direction of motion facilitated via the notion of steepest descent [**11**]. For vehicular systems, the gradient of the total artificial potential field, referred to as the *input force*, determines the speed and direction along which the vehicle moves. The pioneering work on motion planning and control of robots via APFs was carried out by Khatib in [**9**]. Since then many papers utilizing potential fields to address issues such as parking, posture and point stabilities, and path tracking, have appeared. The reader is referred to [**10, 19**] and the references therein for a detailed account of APFs and their applications.

In this paper, we adopt the Lyapunov-based control scheme employed in [**21, 22, 23, 24, 25, 26, 29**] and utilize it to derive continuous, time-invariant, feedback control laws for formation control of a swarm of 2-link mobile manipulators. The scheme guarantees completion of the following subtasks: collision avoidance; goal convergence, cohesion of swarms; satisfying nonholonomic constraints; satisfying kinodynamic constraints (bounds on velocity and steering angle, workspace boundaries); and forcing final desired orientation of the formation.

An observed swarm behavior leads to the concept of *formation stiffness*, which is a rule necessitating a strict observance of the prescribed formation during the motion of the swarm. On one hand, there are *split/rejoin* maneuvers which can be required in applications, for ex-

ample, reconnaissance, sampling and surveillance while, on the other hand, there are *tight-formations* which can be required in applications that require cooperative payload transportation [**3, 4, 8**]. Then there are *low-degree formations* (required in convoying and demining [**20**]) that are strict but do allow for slight distortions. Swarming motions presented in this paper follow the latter approach and encompass slight distortions to cater for collision and obstacle avoidances. This, to the authors knowledge, is carried out for the first time for the control of kinodynamic model of 2-link mobile manipulators in a prescribed formation. To ensure a low-degree formation, the authors included moving ghost targets, inter-robot bounds for aggregation and heading. The resultant controllers inherently allow temporary distortions in the formation in order to avoid obstacles that are directly in the path of the procession. The robots are then forced into constellation where the original formation is re-established before seeking convergence to target. The controllers also guarantee re-establishment of the prescribed formation if a robot is getting closer or lagging behind another robot in the formation.

The new control scheme gives an improved performance in comparison to the behavior-based models, which treat each subtask separately as a behavior and usually run into the problem of overlapping and prioritization.

2. System modeling: The leader-follower scheme. In this paper, we adopt the well known leader-follower scheme. It is a scheme within which the movement of each member of a swarm is with respect to a single individual (leader).

We begin by deriving a dynamic model using Cartesian coordinates for the leader-follower based formation control of a swarm of n 2-link mobile manipulators (2MMs) with one additional 2MM, labeled A_0, acting as the *leader-robot*. The leader-robot is followed by A_i, $i \in \{1, 2, \ldots, n\}$ acting as the ith *follower-robot*. For simplicity, and without any loss of generality, we let each A_i, $i \in \{0, 1, 2, \ldots, n\}$ have the same dimensions.

As depicted in Figure 1, (x_0, y_0) and (x_i, y_i) are the Cartesian coordinates of the end-effector of the leader-robot and the ith follower-robot, respectively; v_0 and v_i are the leader's and the ith follower-robot's linear velocities; θ_{01} and θ_{i1} are the heading directions of their

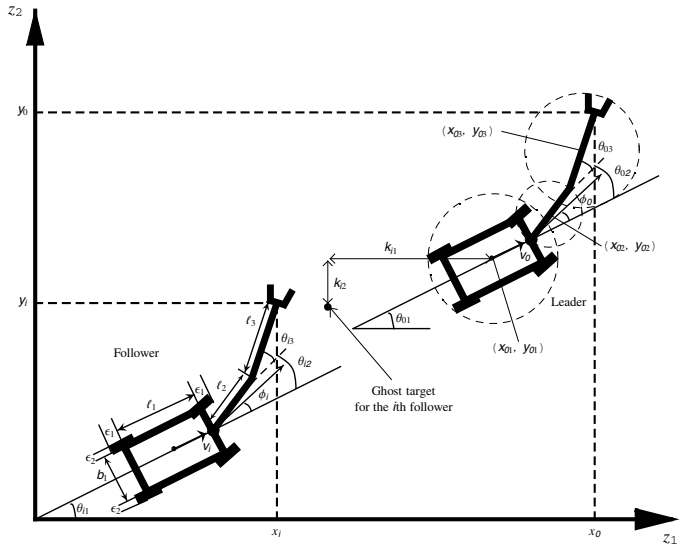

FIGURE 1. Leader-follower scheme of 2-link mobile manipulators.

platforms in global coordinates; θ_{02} and θ_{i2} give the orientations of link 1 with respect to their platforms, while θ_{03} and θ_{i3} give the orientations of link 2 with respect to their link 1. Furthermore, ℓ_1 and b_1 are, respectively, the length and the width of each wheeled platform; while ℓ_2 and ℓ_3 are the lengths of link 1 and link 2, respectively.

Letting $\theta_{iQ} = \theta_{i1} + \theta_{i2}$, $\theta_{iT} = \theta_{i1} + \theta_{i2} + \theta_{i3}$, $\omega_{iQ} = \omega_{i1} + \omega_{i2}$ and $\omega_{iT} = \omega_{i1} + \omega_{i2} + \omega_{i3}$, we can easily derive the dynamic model of the ith 2MM, for $i \in \{0, 1, 2, \ldots, n\}$, as:

$$
\left.
\begin{aligned}
&\dot{x}_i = v_i \cos\theta_{i1} - \ell_1\omega_{i1}\sin\theta_{i1} - \ell_2\omega_{iQ}\sin\theta_{iQ} - \ell_3\omega_{iT}\sin\theta_{iT},\\
&\dot{y}_i = v_i \sin\theta_{i1} + \ell_1\omega_{i1}\cos\theta_{i1} + \ell_2\omega_{iQ}\cos\theta_{iQ} + \ell_3\omega_{iT}\cos\theta_{iT},\\
&\dot{\theta}_{i1} = \omega_{i1}, \qquad \dot{\theta}_{i2} = \omega_{i2}, \qquad \dot{\theta}_{i3} = \omega_{i3},\\
&\dot{v}_i = u_{i1}, \qquad \dot{\omega}_{i1} = u_{i2}, \qquad \dot{\omega}_{i2} = u_{i3}, \qquad \dot{\omega}_{i3} = u_{i4}.
\end{aligned}
\right\} \tag{1}
$$

System (1) is a description of the instantaneous velocities and accelerations of the various bodies of the swarm of 2MMs where the position of the ith 2MM is given as $\mathbf{d}_i = (x_i, y_i)$. We assume that the instantaneous accelerations u_{i1}, u_{i2}, u_{i3} and u_{i4} can move the end-effector of A_i

to its target. In the Lyapunov-based control scheme, $(u_{i1}, u_{i2}, u_{i3}, u_{i4})$ for $i \in \{0, 1, 2, \ldots, n\}$ are considered as the nonlinear controllers for system (1).

We shall use the vector notation $\mathbf{x}_i = (x_i, y_i, \theta_{i1}, \theta_{i2}, \theta_{i3}, v_i, \omega_{i1}, \omega_{i2}, \omega_{i3}) \in \mathbf{R}^9$ in the z_1-z_2 plane to refer to the position and velocity components of the ith 2MM. For generality, we further define $\mathbf{x} = (\mathbf{x}_0, \mathbf{x}_1, \mathbf{x}_2, \ldots \mathbf{x}_n) \in \mathbf{R}^{9\times(n+1)}$.

Now, to ensure that the complete A_i safely steers past an obstacle, we enclose each body of A_i by the smallest possible circle. Given the clearance parameters ε_j for $j = 1, 2, 3$, as shown in Figure 1, we shall enclose the wheeled platform by a protective circular region with radius $r_1 = \sqrt{(\ell_1 + 2\varepsilon_1)^2 + (b_1 + 2\varepsilon_2)^2}/2$, link 1 with radius $r_2 = \ell_2/2$ and link 2 with a radius of $r_3 = \ell_3/2 + \varepsilon_3$. We denote the centers of the wheeled platform, link 1 and link 2 of the ith 2MM as (x_{i1}, y_{i1}), (x_{i2}, y_{i2}) and (x_{i3}, y_{i3}), respectively.

Furthermore, it can be easily verified that the positions of the wheeled platform, link 1 and link 2 of the ith 2MM can be expressed completely in terms of the state space variables x_i, y_i, θ_{i1}, θ_{i2}, and θ_{i3}. Hence for the articulated bodies $m = 1, 2, 3$ of the ith 2MM we have the following functions:

$$\left.\begin{aligned} x_{im} &= x_i - \sum_{k=m}^{3} \frac{\ell_k}{2^{\lfloor m/k \rfloor}} \cos\left(\sum_{p=1}^{k} \theta_{ip}\right), \\ y_{im} &= y_i - \sum_{k=m}^{3} \frac{\ell_k}{2^{\lfloor m/k \rfloor}} \sin\left(\sum_{p=1}^{k} \theta_{ip}\right), \end{aligned}\right\} \tag{2}$$

where $\lfloor m/k \rfloor$ is a floor function. For example, (x_{12}, y_{12}) are the Cartesian coordinates of the center of link 1 of A_1 (1^{st} follower-robot). Note that these position constraints are known as the *holonomic constraints* of the 2MM system.

The Lyapunov-based control scheme requires the construction of a feasible Lyapunov function, which is then utilized to obtain the nonlinear control laws for our kinodynamic system. The control scheme itself operates within the AFP framework. Hence we now design attractive functions that help the swarm move towards its target and avoidance functions that help the swarm in successful collision and obstacle avoidances. We also introduce a new algorithm that establishes

and maintains the formation of the swarm. All these functions will, in a later section, be combined appropriately to form the Lyapunov function.

3. Formation. There have been a number of different approaches designed and employed to establish and maintain robot formations, either of fixed or dynamic topologies. Formations are commonly referenced with respect to the center of mass of the agents [**14, 15**]. Notwithstanding this trend, we make the following assumption to aid in the construction of potential field functions:

Assumption 1. *The prescribed formation is referenced with respect to the end-effectors of the* 2MM*s.*

Now, different degrees of formation stiffness have been addressed in literature; the choice partly due to the nature of the applications [**20**], the collision and obstacle avoidances required, and the overall operational costs involved. In this paper, we desire a significant degree of formation stiffness but allow for slight (but temporary) distortions to help execute the essential collision avoidance maneuvers; this formation is classified as a *low-degree formation*. Instead of adopting concepts such as prioritization and switching, we desire to retain the continuous property of the controllers. Accordingly, we consider a new algorithm that maintains the low-degree formation during the motion.

The algorithm is an amalgamation of the following tasks:

(i) Moving ghost targets;

(ii) Aggregation (inter-robot bounds);

(iii) Heading.

We shall consider these tasks separately to highlight and elucidate the importance of the new technique.

3.1. Moving ghost targets. We introduce the concept of *moving ghost targets*, a variant of the leader-follower scheme, which not only helps in the advancement of formations but also contributes to help maintain these prescribed formations. In the scheme, when the leader A_0 moves towards its target, we want the follower-robots, A_i, $i \in$

$\{1, 2, \ldots, n\}$, to move towards their moving ghost targets positioned relative to the leader-robot. To put the scheme into place, it is necessary to affix a circular target with center (p_{01}, p_{02}) and radius rt_0 for the leader robot A_0 to reach after some time $t > 0$. We will make the following assumptions with respect to leader-follower scheme:

Assumption 2. *The moving ghost targets of the follower-robots are positioned relative to the wheeled platform of the leader-robot in the leader-follower scheme.*

Assumption 3. *Let* $T_i = \{(z_1, z_2) \in \mathbf{R}^2 : (z_1 - p_{i1})^2 + (z_2 - p_{i2})^2 \leq rt_i^2\}$ *be the target of the leader-robot* $i = 0$ *and the follower-robots* $i \in \{1, 2, \ldots, n\}$.

Remark 1. With the inclusion of these assumptions we can then proclaim that the moving ghost target of the ith follower-robot is positioned k_{i1} units horizontal and k_{i2} units vertical off the center of the wheeled platform of the leader-robot (as shown in Figure 1). Also that the center of the moving ghost target of the ith follower-robot is given as $(p_{i1}, p_{i2}) = (x_{01} - k_{i1}, y_{01} - k_{i2})$ for $i = 1, 2, \ldots, n$ in geometrical space.

For attraction to the target and ghost targets we consider the attractive function

$$V_i(\mathbf{x}) = \frac{1}{2}\left[(x_i - p_{i1})^2 + (y_i - p_{i2})^2 + v_i^2 + \omega_{i1}^2 + \omega_{i2}^2 + \omega_{i3}^2\right], \tag{3}$$

for $i \in \{0, 1, 2, \ldots, n\}$. This function is positive for all $\mathbf{x} \in \mathbf{R}^{9\times(n+1)}$. Once a Lyapunov function candidate for system (1) is established, $V_i(\mathbf{x})$ will act as attractor by having the end-effector of ith 2MM move to its designated target.

3.2. Aggregation: Inter-robot bounds. To maintain cohesion of the multi-robots traversing their paths to the target configurations we need the concept of *neighbors*:

Definition 1. Neighbors: Any two 2-link mobile manipulators (A_i and A_j, for $i \neq j$) at any time $t \geq 0$ along the trajectory of the swarm are classified as neighbors if they are part of a prescribed formation.

Remark 2. The definition is justified in swarms with $\|\mathbf{d}_i - \mathbf{d}_j\| < M_{ij}^2$ where $M_{ij} > 0$ is the maximum Euclidian distance between the end-effectors of A_i and A_j. However, increasing the density of 2MMs in a swarm can require different sets of neighbors for different individuals of the swarm in either fixed or dynamic formations.

We next consider inter-robot bounds.

Maximum inter-robot bound: The relative distance between the end-effectors of any two neighbors needs to be bounded. We desire $\|\mathbf{d}_i - \mathbf{d}_j\| < M_{ij}^2$. To satisfy this condition, we design the following obstacle avoidance function

$$R_{ij}(\mathbf{x}) = \frac{1}{2}\left[M_{ij}^2 - (x_i - x_j)^2 - (y_i - y_j)^2\right], \tag{4}$$

for $i, j \in \{0, 1, 2, \ldots, n\}$, $j \neq i$.

Minimum inter-robot bound: To prevent any possible collisions between neighbors a minimum distance between them is also warranted. Now, each solid body of the articulated 2MM has to be treated as an obstacle for the other 2MMs in the workspace. Therefore, for each mth body of A_i, $i \in \{0, 1, 2, \ldots, n\}$, to avoid the uth moving solid body of A_j, $j \in \{0, 1, 2, \ldots, n\}$, $j \neq i$, we shall adopt

$$MO_{muij}(\mathbf{x}) = \frac{1}{2}\left[(x_{im} - x_{ju})^2 + (y_{im} - y_{ju})^2 - (r_m + r_u)^2\right], \tag{5}$$

for $m, u = 1, 2, 3$.

These inter-robot bounds are treated as *artificial obstacles*. To generate repulsive fields around these obstacles we follow [**22, 23**] to design new repulsive potential field functions, which basically are inverse functions that encode the above mentioned positive functions into the corresponding denominators and *tuning parameters* in the numerators. These ratios act to prevent inter-robot collisions and to restrict robots from drifting off and destabilizing the prescribed formation. Manipulation of the tuning parameters associated with functions R_{ij} and MO_{muij} provide an added degree of control of the subtasks and help maintain the desired formation.

Henceforth, for each obstacle, we will construct an appropriate avoidance function that will appear in the denominator of a repulsive potential field function with tuning parameters populating the numerator. These functions will be combined into a Lyapunov function in accordance with the Lyapunov-based control scheme.

3.3. Heading. We desire to keep the orientations of the wheeled platforms of the follower-robots the same as that of the wheeled platform of the leader-robot while they traverse their paths to their final configurations. For this, we introduce another new function $|\theta_{01}-\theta_{i1}| < \varepsilon_{0i}$ where $\varepsilon_{0i} > 0$ is the accepted error in the heading. This function will again be treated as an artificial obstacle in our control scheme. For avoidance, we create an obstacle avoidance function which establishes error bounds on orientations of the platforms of leader and follower robots

$$Q_i(\mathbf{x}) = \frac{1}{2}\left[\varepsilon_{0i}^2 - (\theta_{01} - \theta_{i1})^2\right], \tag{6}$$

for $i \in \{1, 2, \ldots, n\}$. The other advantage of utilizing this function is the fact that it inherently allows for rotations of the prescribed formations.

4. Integrated subtasks. Together with establishing and maintaining prescribed formations, we have included a number of subtasks typically integrated with motion planning and control of autonomous vehicular systems. These subtasks are: final desired orientation of the formation; goal convergence; kinematic constraints (bounded workspace, fixed obstacles, holonomy and nonholonomy); and dynamic constraints (mechanical singularities and modulus bound on velocities). In the following subsections we will discuss these subtasks and design appropriate obstacle avoidance functions.

4.1. Final orientation of formation using a minimum distance technique and ghost walls. A direct result of Brockett's theorem [**2**] is the failure to accomplish stabilizing posture configurations of nonholonomic systems via smooth (even continuous) feedback controllers. Although the final position is reachable, it is difficult to obtain exact orientations at the equilibrium point of this special class of dynamical systems.

In this section, we will use the concepts of *ghost walls* from [**24**] and a minimum distance technique (MDT) from [**23**] to force the prescribed final orientations of the swarm, bearing in mind that the goal reachability has already been guaranteed by the target attractive function designed in subsection 3.1. A useful feature of this methodology is that it works with any desired orientation.

To begin with, we construct ghost walls along the three sides of the target, with the orientations of the walls depending on the final orientations of the swarm. To accomplish the desired orientation of the swarm, we have to avoid these ghost walls. In [**21, 22**], the authors utilized a novel technique, classified as the *obstacle alignment technique*, to avoid these artificial walls; however, the technique became cumbersome once the number of walls erected increased. To retain the simplicity of the controllers we adopt a minimum distance technique.

A minimum distance technique (MDT) utilized in [**21, 23**] gives the distance between the closest point on each kth ghost wall measured perpendicularly from a point on each mth body of A_i. Avoidance of these closest points on a ghost wall at any time $t \geq 0$ essentially results in the avoidance of the entire wall by the entire 2MM.

The parametric representation of this kth ghost wall in the z_1z_2-plane with initial coordinates (a_{k1}, b_{k1}) and final coordinate (a_{k2}, b_{k2}) is

$$c_{imk} = a_{k1} + \lambda_{imk}(a_{k2} - a_{k1}), \qquad d_{imk} = b_{k1} + \lambda_{imk}(b_{k2} - b_{k1}),$$

where $m = 1, 2, 3$ are the three solid bodies of the ith articulated robot. Minimizing the Euclidian distance between the point (x_{im}, y_{im}) and the ghost wall (c_{imk}, d_{imk}), we get

$$\lambda_{imk} = (x_{im} - a_{k1})q_{k1} + (y_{im} - b_{k1})q_{k2}, \text{ for } \lambda_{imk} \in [0, 1],$$

where

$$q_{k1} = \frac{(a_{k2} - a_{k1})}{(a_{k2} - a_{k1})^2 + (b_{k2} - b_{k1})^2}, \quad q_{k2} = \frac{(b_{k2} - b_{k1})}{(a_{k2} - a_{k1})^2 + (b_{k2} - b_{k1})^2}.$$

If $\lambda_{imk} \geq 1$, then we let $\lambda_{imk} = 1$; if $\lambda_{imk} \leq 0$, then we let $\lambda_{imk} = 0$. Otherwise, we accept the value of λ_{imk} between 0 and 1, in which case there is a perpendicular line to the point (c_{imk}, d_{imk}) on the ghost wall from the center (x_{im}, y_{im}) of the mth body of the ith 2MM at every

time $t \geq 0$. We note that each target will be surrounded by three ghost wall lines which have to be avoided by the respective 2MMs. This means that the leader has to avoid the 1st, 2nd and 3rd ghost walls while the ith follower will be avoiding $(3i+1)$, $(3i+2)$ and $(3i+3)$ ghost walls; thus $k \in \{3i+1, 3i+2, 3i+3\}$. The following obstacle avoidance function will ensure that all m bodies of the ith 2MM will avoid their time-varying closest points on the ghost walls surrounding the three sides of the target position

$$LS_{imk}(\mathbf{x}) = \frac{1}{2}\left[(x_{im} - c_{imk})^2 + (y_{im} - d_{imk})^2 - r_m^2\right], \tag{7}$$

for $m = 1, 2, 3$, $k \in \{3i+1, 3i+2, 3i+3\}$ and $i \in \{0, 1, \ldots, n\}$. We again design new repulsive potential field functions as per the procedure outlined in the previous section. The main idea here is to attach necessary and sufficient repulsive potentials to the ghost walls so that the final orientations of all rigid bodies of the 2MMs could be *forced* to eventuate [**21, 23**].

4.2. Auxiliary function. To guarantee that the trajectories of the swarm vanish precisely at the equilibrium state, we design a new auxiliary function that would be multiplied to the inverse of each obstacle avoidance function mentioned in this research. This is in line with the work in [**29**]. The function is

$$F_i(\mathbf{x}) = \frac{1}{2}\left[(x_i - p_{i1})^2 + (y_i - p_{i2})^2 + \sum_{j=1}^{3} \rho_{ij}(\theta_{ij} - p_{ij+2})^2\right], \tag{8}$$

for $i = 0, 1, 2, \ldots, n$. Note that p_{i3}, p_{i4}, p_{i5} are the final orientations of the wheeled platform, link 1 and link 2, respectively, of the ith 2MM. Here $\rho_{i1}, \rho_{i2}, \rho_{i3} > 0$ are new parameters classified as the *angle-gain parameters*, which will be used to force prescribed final orientations of each solid body of the ith 2MM. An angle-gain parameter will have a value of one only if a final orientation is warranted, else it gets a default value of zero.

4.3. Kinematic constraints. The various types of fixed and moving obstacles and their necessary specifications are discussed below. These obstacles are treated as kinematic constraints.

4.3.1. Workspace: Boundary limitations. We consider a planar workspace which is a fixed, closed and bounded rectangular region defined for some $\eta_1 > 2(r_1 + r_2 + r_3)$ and $\eta_2 > 2(r_1 + r_2 + r_3)$, as

$$WS = \{(z_1, z_2) \in \mathbf{R}^2 : 0 \leq z_1 \leq \eta_1, 0 \leq z_2 \leq \eta_2\}.$$

We require the prescribed formation to stay within the rectangular region at all time $t \geq 0$. The boundaries of the region are defined as follows:

(a) Left boundary: $B_1 = \{(z_1, z_2) \in \mathbf{R}^2 : z_1 = 0\}$;

(b) Lower boundary: $B_2 = \{(z_1, z_2) \in \mathbf{R}^2 : z_2 = 0\}$;

(c) Right boundary: $B_3 = \{(z_1, z_2) \in \mathbf{R}^2 : z_1 = \eta_1\}$;

(d) Upper boundary: $B_4 = \{(z_1, z_2) \in \mathbf{R}^2 : z_2 = \eta_2\}$.

In our Lyapunov-based control scheme, these boundaries are considered as *fixed obstacles*, which need to be avoided by each member of the formation. Now, since the two ends of link 1 are protected by the protective circular regions of the wheeled platform and of link 2, respectively, it can be geometrically verified that we need consider obstacle avoidance functions only for the wheeled platform and link 2 of the ith 2MM in order to avoid the workspace boundaries.

Thus, for the avoidance by the wheeled platform we shall adopt the following obstacle avoidance functions [**17**]:

$$W_{i1}(\mathbf{x}) = x_{i1} - r_1, \tag{9a}$$

$$W_{i2}(\mathbf{x}) = y_{i1} - r_1, \tag{9b}$$

$$W_{i3}\mathbf{x}) = \eta_1 - (r_1 + x_{i1}), \tag{9c}$$

$$W_{i4}(\mathbf{x}) = \eta_2 - (r_1 + y_{i1}). \tag{9d}$$

For the avoidance of the left, lower, right and upper boundaries, respectively, by link 2, we shall adopt

$$W_{i5}(\mathbf{x}) = x_{i3} - r_3, \tag{10a}$$

$$W_{i6}(\mathbf{x}) = y_{i3} - r_3, \tag{10b}$$

$$W_{i7}(\mathbf{x}) = \eta_1 - (r_3 + x_{i3}), \tag{10c}$$

$$W_{i8}(\mathbf{x}) = \eta_2 - (r_3 + y_{i3}). \tag{10d}$$

Since $\eta_1 > 2(r_1 + r_2 + r_3)$ and $\eta_2 > 2(r_1 + r_2 + r_3)$, each of the aforementioned functions is positive in WS. That is, $W_{i1}, W_{i3} > 0$ for all $x_{i1} \in (r_1, \eta_1 - r_1)$, $W_{i2}, W_{i4} > 0$ for all $y_{i1} \in (r_1, \eta_2 - r_1)$, $W_{i5}, W_{i7} > 0$ for all $x_{i3} \in (r_3, \eta_1 - r_3)$, and $W_{i6}, W_{i8} > 0$ for all $y_{i3} \in (r_3, \eta_2 - r_3)$, for $i = 1, 2, \ldots, n$, recalling that the forms of (x_{i1}, y_{i1}) and (x_{i3}, y_{i3}) are given in (2).

These obstacle avoidance functions will be appropriately coupled with tuning parameters to obtain the repulsive potentials.

4.3.2. Avoidance of fixed obstacles. Let us fix q obstacles within the boundaries of the workspace. We assume that the lth fixed obstacle is circular with center given as (o_{l1}, o_{l2}) and radius rad_l. We define the lth obstacle as

$$O_l = \{(z_1, z_2) \in \mathbf{R}^2 : (z_1 - o_{l1})^2 + (z_2 - o_{l2})^2 \leq rad_l^2\},$$

for $l = 1, 2, \ldots, q$. For its avoidance, we will need to have separate avoidance functions for each mth body of the ith 2MM. Thus we consider

$$FO_{iml}(\mathbf{x}) = \frac{1}{2}\left[(x_{im} - o_{l1})^2 + (y_{im} - o_{l2})^2 - (r_m + rad_l)^2\right], \tag{11}$$

for $m = 1, 2, 3$, $l = 1, 2, \ldots, q$ and $i = 0, 1, \ldots, n$.

4.4. Dynamic constraints. The motion of a mechanical system restricted due to the presence of a number of self-inflicted and user-inflicted conditions. The self-inflicted conditions are conditions imposed on a system due to its mechanical structure. They predominantly consist of the mechanical singularities of the robotic system. On the other hand, the user-inflicted conditions are conditions imposed on the robotic system with safety in mind. They largely comprise modulus bounds on velocity components, inter-robot bounds and heading of the robot formations [**21**].

Now, the only way these conditions can be incorporated into the Lyapunov-based control scheme is to treat them as obstacles, henceforth classified as *artificial obstacles*. These obstacles will then have to be avoided, in accordance with the Lyapunov-based control scheme.

4.4.1. Mechanical singularities.

(i) Singular configurations arise when $\theta_{i3} = 0$, $\theta_{i3} = \pi$ or $\theta_{i3} = -\pi$. Subsequently, the condition placed on θ_{i3} is $0 < |\theta_{i3}| < \pi$ for $\theta_{i3} \in (-\pi, 0) \cup (0, \pi)$, which implies that the links can neither be fully stretched nor be folded back [**29**];

(ii) The angle between link 1 and the platform is bounded by $-\pi/2 < \theta_{i2} < \pi/2$. In other words, link 1 of the ith 2MM can only freely rotate within $(-\pi/2, \pi/2)$.

For the avoidance of artificial obstacles created from the aforementioned singular configurations and the restriction on θ_{i2}, we will adopt the following avoidance functions:

$$S_{i1}(\mathbf{x}) = |\theta_{i3}|; \tag{12a}$$

$$S_{i2}(\mathbf{x}) = \pi - |\theta_{i3}|; \tag{12b}$$

$$S_{i3}(\mathbf{x}) = \frac{1}{2}\left(\frac{\pi}{2} - \theta_{i2}\right)\left(\frac{\pi}{2} + \theta_{i2}\right). \tag{12c}$$

4.4.2. Modulus bound on velocities. From a practical viewpoint, the translational and rotational velocities of the 2MMs are bounded, so we include the following additional constraints:

(i) $|v_i| < v_{\max}$, where $v_{\max}$ is the *maximal achievable speed*;

(ii) $|\omega_{i1}| < v_{\max}/|\rho_{\min}|$, where $\rho_{\min} = \ell_1/\tan(\phi_{\max})$. This condition arises due to the boundness of the steering angle, ϕ_i. That is $|\phi_i| \leq \phi_{\max}$, where $\phi_{\max}$ is *maximal steering angle*;

(iii) $|\omega_{i2}| < \omega_{2\max}$ and $|\omega_{i3}| < \omega_{3\max}$, where $\omega_{2\max}$, $\omega_{3\max}$ are the *maximal rotational velocities* of link 1 and link 2 respectively.

For the avoidance of these new artificial obstacles, we will adopt the following avoidance functions, for $i = 0, 1, 2, \ldots, n$:

$$U_{i1}(\mathbf{x}) = \frac{1}{2}\left(v_{\max}^2 - v_i^2\right), \tag{13a}$$

$$U_{i2}(\mathbf{x}) = \frac{1}{2}\left(\frac{v_{\max}^2}{\rho_{\min}^2} - \omega_{i1}^2\right), \tag{13b}$$

$$U_{i3}(\mathbf{x}) = \frac{1}{2}\left(\omega_{2\max}^2 - \omega_{i2}^2\right), \tag{13c}$$

$$U_{i4}(\mathbf{x}) = \frac{1}{2}\left(\omega_{3\max}^2 - \omega_{i3}^2\right). \tag{13d}$$

When used appropriately in a Lyapunov function, these positive functions will help in the avoidance of the artificial obstacles and therefore guarantee adherence to the limitations placed upon the steering angle and the velocities.

5. Lyapunov-based control scheme. We shall now define a Lyapunov function candidate and then utilize it to extract the nonlinear control laws for our system (1).

5.1. Lyapunov function candidate. Combining all the target attractive and obstacle avoidance functions (3)–(13) and introducing tuning parameters, $\alpha_{is} > 0$, $\xi_{ip} > 0$, $\gamma_{iml} > 0$, $\sigma_i > 0$, $\zeta_{imk} > 0$, $\beta_{ir} > 0$, $\psi_{ij} > 0$ and $\varphi_{muij} > 0$, we define a Lyapunov function candidate for system (1) (suppressing $\mathbf{x}$) as

$$
\begin{aligned}
L_{(1)} = \sum_{i=0}^{n} \Bigg\{ V_i + F_i \Bigg[& \sum_{s=1}^{8} \frac{\alpha_{is}}{W_{is}} \\
& + \sum_{m=1}^{3} \Bigg(\sum_{l=1}^{q} \frac{\gamma_{iml}}{FO_{iml}} + \sum_{k=3i+1}^{3i+3} \frac{\zeta_{imk}}{LS_{imk}} \Bigg) \\
& + \sum_{r=1}^{4} \frac{\beta_{ir}}{U_{ir}} + \sum_{p=1}^{3} \frac{\xi_{ip}}{S_{ip}} \\
& + \sum_{\substack{j=0 \\ j \neq i}}^{n} \Bigg(\sum_{m=1}^{3} \sum_{u=1}^{3} \frac{\varphi_{muij}}{MO_{muij}} + \frac{\psi_{ij}}{R_{ij}} \Bigg) \Bigg] \Bigg\} \\
& + \sum_{i=1}^{n} \frac{\sigma_i F_i}{Q_i}.
\end{aligned} \tag{14}
$$

5.2. Controller design. Taking the time derivative of the Lyapunov function candidate and treating the state variable separately, we get the semi-negative definite form

$$
\dot{L}_{(1)}(\mathbf{x}) = -\sum_{i=0}^{n} \left(\delta_{i1} v_i^2 + \delta_{i2} \omega_{i1}^2 + \delta_{i3} \omega_{i2}^2 + \delta_{i4} \omega_{i3}^2 \right) \leq 0,
$$

provided our feedback nonlinear controllers are given as

(15)

$$
\left.
\begin{aligned}
u_{i1} &= -\left[\delta_{i1} v_i + (f_{i1} + f_{i3} + f_{i5} + f_{i7}) \cos\theta_{i1} \right.\\
&\quad \left. + (f_{i2} + f_{i4} + f_{i6} + f_{i8}) \sin\theta_{i1}\right] / g_{i4},\\
u_{i2} &= -\Bigg[\delta_{i2}\omega_{i1} - \left(f_{i1} + \frac{1}{2} f_{i3} + f_{i5} + f_{i7}\right)\ell_1 \sin\theta_{i1}\\
&\quad + \left(f_{i2} + \frac{1}{2} f_{i4} + f_{i6} + f_{i8}\right)\ell_1 \cos\theta_{i1}\\
&\quad - \left(f_{i1} + \frac{1}{2} f_{i5} + f_{i7}\right)\ell_2 \sin\theta_{iQ}\\
&\quad + \left(f_{i2} + \frac{1}{2} f_{i6} + f_{i8}\right)\ell_2 \cos\theta_{iQ}\\
&\quad - \left(f_{i1} + \frac{1}{2} f_{i7}\right)\ell_3 \sin\theta_{iT}\\
&\quad + \left(f_{i2} + \frac{1}{2} f_{i8}\right)\ell_3 \cos\theta_{iT} + g_{i1}\Bigg] \Big/ g_{i5},\\
u_{i3} &= -\Bigg[\delta_{i3}\omega_{i2} - \left(f_{i1} + \frac{1}{2} f_{i5} + f_{i7}\right)\ell_2 \sin\theta_{iQ}\\
&\quad + \left(f_{i2} + \frac{1}{2} f_{i6} + f_{i8}\right)\ell_2 \cos\theta_{iQ}\\
&\quad - \left(f_{i1} + \frac{1}{2} f_{i7}\right)\ell_3 \sin\theta_{iT} + \left(f_{i2} + \frac{1}{2} f_{i8}\right)\ell_3 \cos\theta_{iT} + g_{i2}\Bigg] \Big/ g_{i6},\\
u_{i4} &= -\Bigg[\delta_{i4}\omega_{i3} - \left(f_{i1} + \frac{1}{2} f_{i7}\right)\ell_3 \sin\theta_{iT}\\
&\quad + \left(f_{i2} + \frac{1}{2} f_{i8}\right)\ell_3 \cos\theta_{iT} + g_{i3}\Bigg] \Big/ g_{i7},
\end{aligned}
\right\}
$$

where: δ_{ij}, for $i \in \{1, 2, \ldots, n\}$ and $j \in \{1, 2, \ldots, 4\}$ are positive constants classified as *convergence parameters*, the functions $f_{01}, f_{02}, \ldots, f_{08}$ and $g_{01}, g_{02}, \ldots, g_{07}$ for the leader-robot are defined as

$$
f_{01} = \left[1 + \sum_{s=1}^{8} \frac{\alpha_{0s}}{W_{0s}} + \sum_{p=1}^{3} \frac{\xi_{0p}}{S_{0p}} + \sum_{m=1}^{3} \left(\sum_{l=1}^{q} \frac{\gamma_{0ml}}{FO_{0ml}} + \sum_{k=1}^{3} \frac{\zeta_{0mk}}{LS_{0mk}} \right)\right.
$$

$$
\begin{aligned}
&+\sum_{r=1}^{4}\frac{\beta_{0r}}{U_{0r}}+\sum_{j=1}^{n}\left(\sum_{m=1}^{3}\sum_{u=1}^{3}\frac{\varphi_{mu0j}}{MO_{mu0j}}+\frac{\psi_{0j}}{R_{0j}}\right)\Bigg](x_0-p_{01})\\
&+F_0\sum_{j=1}^{n}\frac{\psi_{0j}}{R_{0j}^2}(x_0-x_j)-\sum_{i=1}^{n}\frac{F_i\psi_{i0}}{R_{i0}^2}(x_i-x_0),\\
f_{03}=&-F_0\left\{\frac{\alpha_{01}}{W_{01}^2}-\frac{\alpha_{03}}{W_{03}^2}+\sum_{l=1}^{q}\frac{\gamma_{01l}}{FO_{01l}^2}\,(x_{01}-o_{l1})\right\}\\
&-\sum_{j=1}^{n}\sum_{u=1}^{3}\left(\frac{\varphi_{1u0j}F_i}{MO_{1u0j}^2}+\frac{\varphi_{1uj0}F_j}{MO_{1uj0}^2}\right)(x_{01}-x_{ju})\\
&-\sum_{k=1}^{3}\frac{\psi_{01k}F_0}{LS_{01k}^2}\Big[(1-(a_{k2}-a_{k1})q_{k1})\,(x_{01}-c_{01k})\\
&-(b_{k2}-b_{k1})q_{k1}\,(y_{01}-d_{01k})\Big]\\
&-\sum_{i=1}^{n}\Bigg[1+\sum_{s=1}^{8}\frac{\alpha_{is}}{W_{is}}+\sum_{p=1}^{3}\frac{\xi_{ip}}{S_{ip}}\\
&+\sum_{m=1}^{3}\left(\sum_{l=1}^{q}\frac{\gamma_{iml}}{FO_{iml}}+\sum_{k=3i+1}^{3i+3}\frac{\zeta_{imk}}{LS_{imk}}\right)\\
&+\sum_{r=1}^{4}\frac{\beta_{ir}}{U_{ir}}+\sum_{\substack{j=0\\j\neq i}}^{n}\left(\sum_{m=1}^{3}\sum_{u=1}^{3}\frac{\varphi_{muij}}{MO_{muij}}+\frac{\psi_{ij}}{R_{ij}}\right)\Bigg](x_i-(x_{01}-k_{i1})),\\
f_{02}=&\Bigg[1+\sum_{s=1}^{8}\frac{\alpha_{0s}}{W_{0s}}+\sum_{p=1}^{3}\frac{\xi_{0p}}{S_{0p}}\\
&+\sum_{m=1}^{3}\left(\sum_{l=1}^{q}\frac{\gamma_{0ml}}{FO_{0ml}}+\sum_{k=1}^{3}\frac{\zeta_{0mk}}{LS_{0mk}}\right)+\sum_{r=1}^{4}\frac{\beta_{0r}}{U_{0r}}\\
&+\sum_{j=1}^{n}\left(\sum_{m=1}^{3}\sum_{u=1}^{3}\frac{\varphi_{mu0j}}{MO_{mu0j}}+\frac{\psi_{0j}}{R_{0j}}\right)\Bigg](y_0-p_{02})\\
&+F_0\sum_{j=1}^{n}\frac{\psi_{0j}}{R_{0j}^2}(x_0-x_j)-\sum_{i=1}^{n}\frac{F_i\psi_{i0}}{R_{i0}^2}(x_i-x_0),
\end{aligned}
$$

$$
\begin{aligned}
f_{04} = &-F_0\left\{ \frac{\alpha_{02}}{W_{02}^2} - \frac{\alpha_{04}}{W_{04}^2} + \sum_{l=1}^{q} \frac{\gamma_{01l}}{FO_{01l}^2}\,(y_{01} - o_{l2}) \right\} \\
&- \sum_{j=1}^{n}\sum_{u=1}^{3} \left(\frac{\varphi_{1u0j}F_i}{MO_{1u0j}^2} + \frac{\varphi_{1uj0}F_j}{MO_{1uj0}^2} \right)(y_{01} - y_{ju}) \\
&- \sum_{k=1}^{3} \frac{\psi_{01k}F_0}{LS_{01k}^2}\Big[(1 - (b_{k2} - b_{k1})q_{k2})\,(y_{01} - d_{01k}) \\
&- (a_{k2} - a_{k1})q_{k2}\,(x_{01} - c_{01k}) \Big] \\
&- \sum_{i=1}^{n} \Bigg[1 + \sum_{s=1}^{8} \frac{\alpha_{is}}{W_{is}} + \sum_{p=1}^{3} \frac{\xi_{ip}}{S_{ip}} \\
&+ \sum_{m=1}^{3} \left(\sum_{l=1}^{q} \frac{\gamma_{iml}}{FO_{iml}} + \sum_{k=3i+1}^{3i+3} \frac{\zeta_{imk}}{LS_{imk}} \right) \\
&+ \sum_{r=1}^{4} \frac{\beta_{ir}}{U_{ir}} + \sum_{\substack{j=0 \\ j\neq i}}^{n} \left(\sum_{m=1}^{3}\sum_{u=1}^{3} \frac{\varphi_{muij}}{MO_{muij}} + \frac{\psi_{ij}}{R_{ij}} \right) \Bigg] (y_i - (y_{01} - k_{i2})), \\
f_{05} = &- \sum_{l=1}^{q} \frac{\gamma_{02l}F_0}{FO_{02l}^2}\,(x_{02} - o_{l1}) \\
&- \sum_{j=1}^{n}\sum_{u=1}^{3} \left(\frac{\varphi_{2u0j}F_i}{MO_{2u0j}^2} + \frac{\varphi_{2uj0}F_j}{MO_{2uj0}^2} \right)(x_{02} - x_{ju}) \\
&- \sum_{k=1}^{3} \frac{\psi_{02k}F_0}{LS_{02k}^2}\Big[(1 - (a_{k2} - a_{k1})q_{k1})\,(x_{02} - c_{02k}) \\
&- (b_{k2} - b_{k1})q_{k1}\,(y_{02} - d_{02k}) \Big], \\
f_{06} = &- \sum_{l=1}^{q} \frac{\gamma_{02l}F_0}{FO_{02l}^2}\,(y_{02} - o_{l2}) \\
&- \sum_{j=1}^{n}\sum_{u=1}^{3} \left(\frac{\varphi_{2u0j}F_0}{MO_{2u0j}^2} + \frac{\varphi_{2uj0}F_j}{MO_{2uj0}^2} \right)(y_{02} - y_{ju}) \\
&- \sum_{k=1}^{3} \frac{\psi_{02k}F_0}{LS_{02k}^2}\Big[(1 - (b_{k2} - b_{k1})q_{k2})\,(y_{02} - d_{02k})
\end{aligned}
$$

$$
\begin{aligned}
&\quad - (a_{k2} - a_{k1}) q_{k2} \left(x_{02} - c_{02k}\right) \Big], \\
f_{07} &= -F_0 \left\{ \frac{\alpha_{05}}{W_{05}^2} - \frac{\alpha_{07}}{W_{07}^2} + \sum_{l=1}^{q} \frac{\gamma_{03l}}{FO_{03l}^2} \left(x_{03} - o_{l1}\right) \right\} \\
&\quad - \sum_{j=1}^{n} \sum_{u=1}^{3} \left(\frac{\varphi_{3u0j} F_i}{MO_{3u0j}^2} + \frac{\varphi_{3uj0} F_j}{MO_{3uj0}^2} \right) \left(x_{03} - x_{ju}\right) \\
&\quad - \sum_{k=1}^{3} \frac{\psi_{03k} F_0}{LS_{03k}^2} \Big[\left(1 - (a_{k2} - a_{k1}) q_{k1}\right) \left(x_{03} - c_{03k}\right) \\
&\quad - (b_{k2} - b_{k1}) q_{k1} \left(y_{03} - d_{03k}\right) \Big], \\
f_{08} &= -F_0 \left\{ \frac{\alpha_{06}}{W_{06}^2} - \frac{\alpha_{08}}{W_{08}^2} + \sum_{l=1}^{q} \frac{\gamma_{03l}}{FO_{03l}^2} \left(y_{03} - o_{l2}\right) \right\} \\
&\quad - \sum_{j=1}^{n} \sum_{u=1}^{3} \left(\frac{\varphi_{3u0j} F_0}{MO_{3u0j}^2} + \frac{\varphi_{3uj0} F_j}{MO_{3uj0}^2} \right) \left(y_{03} - y_{ju}\right) \\
&\quad - \sum_{k=1}^{3} \frac{\psi_{03k} F_0}{LS_{03k}^2} \Big[\left(1 - (b_{k2} - b_{k1}) q_{k2}\right) \left(y_{03} - d_{03k}\right) \\
&\quad - (a_{k2} - a_{k1}) q_{k2} \left(x_{03} - c_{03k}\right) \Big], \\
g_{01} &= \Big[\sum_{s=1}^{8} \frac{\alpha_{0s}}{W_{0s}} + \sum_{p=1}^{3} \frac{\xi_{0p}}{S_{0p}} \\
&\quad + \sum_{m=1}^{3} \left(\sum_{l=1}^{q} \frac{\gamma_{0ml}}{FO_{0ml}} + \sum_{k=1}^{3} \frac{\zeta_{0mk}}{LS_{0mk}} \right) \\
&\quad + \sum_{r=1}^{4} \frac{\beta_{0r}}{U_{0r}} + \sum_{j=1}^{n} \left(\sum_{m=1}^{3} \sum_{u=1}^{3} \frac{\varphi_{mu0j}}{MO_{mu0j}} + \frac{\psi_{0j}}{R_{0j}} \right) \Big] \rho_{01} (\theta_{01} - p_{03}) \\
&\quad + \sum_{i=1}^{n} \frac{\sigma_i F_i}{Q_i^2} (\theta_{01} - \theta_{i1}), \\
g_{02} &= \Big[\sum_{s=1}^{8} \frac{\alpha_{0s}}{W_{0s}} + \sum_{p=1}^{3} \frac{\xi_{0p}}{S_{0p}} + \sum_{m=1}^{3} \left(\sum_{l=1}^{q} \frac{\gamma_{0ml}}{FO_{0ml}} + \sum_{k=1}^{3} \frac{\zeta_{0mk}}{LS_{0mk}} \right)
\end{aligned}
$$

$$
\begin{aligned}
&+\sum_{r=1}^{4}\frac{\beta_{0r}}{U_{0r}}+\sum_{j=1}^{n}\left(\sum_{m=1}^{3}\sum_{u=1}^{3}\frac{\varphi_{mu0j}}{MO_{mu0j}}+\frac{\psi_{0j}}{R_{0j}}\right)\Bigg]\\
&\times\rho_{02}(\theta_{02}-p_{04})+\frac{\xi_{03}F_0}{S_{03}^2}\theta_{02},\\
g_{03}=&\left[\sum_{s=1}^{8}\frac{\alpha_{0s}}{W_{0s}}+\sum_{p=1}^{3}\frac{\xi_{0p}}{S_{0p}}+\sum_{m=1}^{3}\left(\sum_{l=1}^{q}\frac{\gamma_{0ml}}{FO_{0ml}}+\sum_{k=1}^{3}\frac{\zeta_{0mk}}{LS_{0mk}}\right)\right.\\
&\left.+\sum_{r=1}^{4}\frac{\beta_{0r}}{U_{0r}}+\sum_{j=1}^{n}\left(\sum_{m=1}^{3}\sum_{u=1}^{3}\frac{\varphi_{mu0j}}{MO_{mu0j}}+\frac{\psi_{0j}}{R_{0j}}\right)\right]\rho_{03}(\theta_{03}-p_{05})\\
&-F_0\left(\frac{\xi_{01}}{S_{01}^2}-\frac{\xi_{02}}{S_{02}^2}\right)\left(\frac{|\theta_{03}|}{\theta_{03}}\right),\\
g_{04}=1+\frac{\beta_{01}F_0}{U_{01}^2},&\qquad g_{05}=1+\frac{\beta_{02}F_0}{U_{02}^2},\\
g_{06}=1+\frac{\beta_{03}F_0}{U_{03}^2},&\qquad g_{07}=1+\frac{\beta_{04}F_0}{U_{04}^2}.
\end{aligned}
$$

The functions $f_{i1}, f_{i2}, \ldots, f_{i8}$ and $g_{i1}, g_{i2}, \ldots, g_{i7}$ for the ith follower-robot are defined as

$$
\begin{aligned}
f_{i1}=&\left[1+\sum_{s=1}^{8}\frac{\alpha_{is}}{W_{is}}+\sum_{p=1}^{3}\frac{\xi_{ip}}{S_{ip}}+\sum_{m=1}^{3}\left(\sum_{l=1}^{q}\frac{\gamma_{iml}}{FO_{iml}}+\sum_{k=3i+1}^{3i+3}\frac{\zeta_{imk}}{LS_{imk}}\right)\right.\\
&\left.+\sum_{r=1}^{4}\frac{\beta_{ir}}{U_{ir}}+\frac{\sigma_i}{Q_i}+\sum_{\substack{j=0\\ j\neq i}}^{n}\left(\sum_{m=1}^{3}\sum_{u=1}^{3}\frac{\varphi_{muij}}{MO_{muij}}+\frac{\psi_{ij}}{R_{ij}}\right)\right](x_i-(x_{01}-k_{i1}))\\
&+\sum_{\substack{j=0\\ j\neq i}}^{n}\left(\frac{F_i\psi_{ij}}{R_{ij}^2}+\frac{F_j\psi_{ji}}{R_{ji}^2}\right)(x_i-x_j),\\
f_{i2}=&\left[1+\sum_{s=1}^{8}\frac{\alpha_{is}}{W_{is}}+\sum_{p=1}^{3}\frac{\xi_{ip}}{S_{ip}}+\sum_{m=1}^{3}\left(\sum_{l=1}^{q}\frac{\gamma_{iml}}{FO_{iml}}+\sum_{k=3i+1}^{3i+3}\frac{\zeta_{imk}}{LS_{imk}}\right)\right.\\
&\left.+\sum_{r=1}^{4}\frac{\beta_{ir}}{U_{ir}}+\frac{\sigma_i}{Q_i}+\sum_{\substack{j=0\\ j\neq i}}^{n}\left(\sum_{m=1}^{3}\sum_{u=1}^{3}\frac{\varphi_{muij}}{MO_{muij}}+\frac{\psi_{ij}}{R_{ij}}\right)\right](y_i-(y_{01}-k_{i2}))
\end{aligned}
$$

$$+\sum_{\substack{j=0\\j\neq i}}^{n}\left(\frac{F_i\psi_{ij}}{R_{ij}^2}+\frac{F_j\psi_{ji}}{R_{ji}^2}\right)(y_i-y_j),$$

$$f_{i3}=-F_i\left\{\frac{\alpha_{i1}}{W_{i1}^2}-\frac{\alpha_{i3}}{W_{i3}^2}+\sum_{l=1}^{q}\frac{\gamma_{i1l}}{FO_{i1l}^2}\,(x_{i1}-o_{l1})\right\}$$
$$-\sum_{\substack{j=0\\j\neq i}}^{n}\sum_{u=1}^{3}\left(\frac{\varphi_{1uij}F_i}{MO_{1uij}^2}+\frac{\varphi_{1uji}F_j}{MO_{1uji}^2}\right)(x_{i1}-x_{ju})$$
$$-\sum_{k=3i+1}^{3i+3}\frac{\psi_{i1k}F_i}{LS_{i1k}^2}\Big[(1-(a_{k2}-a_{k1})q_{k1})\,(x_{i1}-c_{i1k})$$
$$-(b_{k2}-b_{k1})q_{k1}\,(y_{i1}-d_{i1k})\Big],$$

$$f_{i4}=-F_i\left\{\frac{\alpha_{i2}}{W_{i2}^2}-\frac{\alpha_{i4}}{W_{i4}^2}+\sum_{l=1}^{q}\frac{\gamma_{i1l}}{FO_{i1l}^2}\,(y_{i1}-o_{l2})\right\}$$
$$-\sum_{\substack{j=0\\j\neq i}}^{n}\sum_{u=1}^{3}\left(\frac{\varphi_{1uij}F_i}{MO_{1uij}^2}+\frac{\varphi_{1uji}F_j}{MO_{1uji}^2}\right)(y_{i1}-y_{ju})$$
$$-\sum_{k=3i+1}^{3i+3}\frac{\psi_{i1k}F_i}{LS_{i1k}^2}\Big[(1-(b_{k2}-b_{k1})q_{k2})\,(y_{i1}-d_{i1k})$$
$$-(a_{k2}-a_{k1})q_{k2}\,(x_{i1}-c_{i1k})\Big],$$

$$f_{i5}=-\sum_{l=1}^{q}\frac{\gamma_{i2l}F_i}{FO_{i2l}^2}\,(x_{i2}-o_{l1})-\sum_{\substack{j=0\\j\neq i}}^{n}\sum_{u=1}^{3}\left(\frac{\varphi_{2uij}F_i}{MO_{2uij}^2}+\frac{\varphi_{2uji}F_j}{MO_{2uji}^2}\right)(x_{i2}-x_{ju})$$
$$-\sum_{k=3i+1}^{3i+3}\frac{\psi_{i2k}F_i}{LS_{i2k}^2}\Big[(1-(a_{k2}-a_{k1})q_{k1})\,(x_{i2}-c_{i2k})$$
$$-(b_{k2}-b_{k1})q_{k1}\,(y_{i2}-d_{i2k})\Big],$$

$$f_{i6}=-\sum_{l=1}^{q}\frac{\gamma_{i2l}F_i}{FO_{i2l}^2}\,(y_{i2}-o_{l2})-\sum_{\substack{j=0\\j\neq i}}^{n}\sum_{u=1}^{3}\left(\frac{\varphi_{2uij}F_i}{MO_{2uij}^2}+\frac{\varphi_{2uji}F_j}{MO_{2uji}^2}\right)(y_{i2}-y_{ju})$$

$$
\begin{aligned}
&- \sum_{k=3i+1}^{3i+3} \frac{\psi_{i2k}F_i}{LS_{i2k}^2}\Big[(1-(b_{k2}-b_{k1})q_{k2})\,(y_{i2}-d_{i2k}) \\
&- (a_{k2}-a_{k1})q_{k2}\,(x_{i2}-c_{i2k})\Big], \\
f_{i7} = &-F_i\Big\{\frac{\alpha_{i5}}{W_{i5}^2} - \frac{\alpha_{i7}}{W_{i7}^2} + \sum_{l=1}^{q}\frac{\gamma_{i3l}}{FO_{i3l}^2}\,(x_{i3}-o_{l1})\Big\} \\
&- \sum_{\substack{j=0\\ j\neq i}}^{n}\sum_{u=1}^{3}\left(\frac{\varphi_{3uij}F_i}{MO_{3uij}^2} + \frac{\varphi_{3uji}F_j}{MO_{3uji}^2}\right)(x_{i3}-x_{ju}) \\
&- \sum_{k=3i+1}^{3i+3} \frac{\psi_{i3k}F_i}{LS_{i3k}^2}\Big[(1-(a_{k2}-a_{k1})q_{k1})\,(x_{i3}-c_{i3k}) \\
&- (b_{k2}-b_{k1})q_{k1}\,(y_{i3}-d_{i3k})\Big], \\
f_{i8} = &-F_i\Big\{\frac{\alpha_{i6}}{W_{i6}^2} - \frac{\alpha_{i8}}{W_{i8}^2} + \sum_{l=1}^{q}\frac{\gamma_{i3l}}{FO_{i3l}^2}\,(y_{i3}-o_{l2})\Big\} \\
&- \sum_{\substack{j=0\\ j\neq i}}^{n}\sum_{u=1}^{3}\left(\frac{\varphi_{3uij}F_i}{MO_{3uij}^2} + \frac{\varphi_{3uji}F_j}{MO_{3uji}^2}\right)(y_{i3}-y_{ju}) \\
&- \sum_{k=3i+1}^{3i+3} \frac{\psi_{i3k}F_i}{LS_{i3k}^2}\Big[(1-(b_{k2}-b_{k1})q_{k2})\,(y_{i3}-d_{i3k}) \\
&- (a_{k2}-a_{k1})q_{k2}\,(x_{i3}-c_{i3k})\Big], \\
g_{i1} = &\Big[\sum_{s=1}^{8}\frac{\alpha_{is}}{W_{is}} + \sum_{p=1}^{3}\frac{\xi_{ip}}{S_{ip}} + \sum_{m=1}^{3}\left(\sum_{l=1}^{q}\frac{\gamma_{iml}}{FO_{iml}} + \sum_{k=3i+1}^{3i+3}\frac{\zeta_{imk}}{LS_{imk}}\right) \\
&+\sum_{r=1}^{4}\frac{\beta_{ir}}{U_{ir}} + \frac{\sigma_i}{Q_i} + \sum_{\substack{j=0\\ j\neq i}}^{n}\left(\sum_{m=1}^{3}\sum_{u=1}^{3}\frac{\varphi_{muij}}{MO_{muij}} + \frac{\psi_{ij}}{R_{ij}}\right)\Big]\rho_{i1}(\theta_{i1}-p_{i3}) \\
&- \frac{\sigma_i F_i}{Q_i^2}(\theta_{01}-\theta_{i1}), \\
g_{i2} = &\Big[\sum_{s=1}^{8}\frac{\alpha_{is}}{W_{is}} + \sum_{p=1}^{3}\frac{\xi_{ip}}{S_{ip}} + \sum_{m=1}^{3}\left(\sum_{l=1}^{q}\frac{\gamma_{iml}}{FO_{iml}} + \sum_{k=3i+1}^{3i+3}\frac{\zeta_{imk}}{LS_{imk}}\right)
\end{aligned}
$$

$$+\sum_{r=1}^{4}\frac{\beta_{ir}}{U_{ir}}+\frac{\sigma_i}{Q_i}+\sum_{\substack{j=0\\ j\neq i}}^{n}\left(\sum_{m=1}^{3}\sum_{u=1}^{3}\frac{\varphi_{muij}}{MO_{muij}}+\frac{\psi_{ij}}{R_{ij}}\right)\Bigg]\rho_{i2}(\theta_{i2}-p_{i4})$$

$$+\frac{\xi_{i3}F_i}{S_{i3}^2}\theta_{i2},$$

$$g_{i3}=\Bigg[\sum_{s=1}^{8}\frac{\alpha_{is}}{W_{is}}+\sum_{p=1}^{3}\frac{\xi_{ip}}{S_{ip}}+\sum_{m=1}^{3}\left(\sum_{l=1}^{q}\frac{\gamma_{iml}}{FO_{iml}}+\sum_{k=3i+1}^{3i+3}\frac{\zeta_{imk}}{LS_{imk}}\right)$$

$$+\sum_{r=1}^{4}\frac{\beta_{ir}}{U_{ir}}+\frac{\sigma_i}{Q_i}+\sum_{\substack{j=0\\ j\neq i}}^{n}\left(\sum_{m=1}^{3}\sum_{u=1}^{3}\frac{\varphi_{muij}}{MO_{muij}}+\frac{\psi_{ij}}{R_{ij}}\right)\Bigg]\rho_{i3}(\theta_{i3}-p_{i5})$$

$$-F_i\left(\frac{\xi_{i1}}{S_{i1}^2}-\frac{\xi_{i2}}{S_{i2}^2}\right)\left(\frac{|\theta_{i3}|}{\theta_{i3}}\right),$$

$$g_{i4}=1+\frac{\beta_{i1}F_i}{U_{i1}^2},\qquad g_{i5}=1+\frac{\beta_{i2}F_i}{U_{i2}^2},$$

$$g_{i6}=1+\frac{\beta_{i3}F_i}{U_{i3}^2},\qquad g_{i7}=1+\frac{\beta_{i4}F_i}{U_{i4}^2}.$$

5.3. Stability analysis. Define $\mathbf{x}_i^*=(p_{i1},p_{i2},\theta_{i1},\theta_{i2},\theta_{i3},0,0,0,0)\in\mathbf{R}^9\in D(L)$. Then, given the controllers (15), it can be verified that $\mathbf{x}_e=(\mathbf{x}_0^*,\mathbf{x}_1^*,\mathbf{x}_2^*,\dots\mathbf{x}_n^*)\in D(L)$ as an equilibrium state for system (1).

Now, since the Lyapunov function candidate $L(\mathbf{x})$ for system (1) is defined, continuous and positive over the domain

$$\begin{aligned}D(L)(\mathbf{x})=\{\mathbf{x}\in\mathbf{R}^{9\times(n+1)}:\ & W_{is}(\mathbf{x})>0,\quad s=1,\dots,8;\\ & S_{ip}(\mathbf{x})>0,\quad p=1,2,3;\\ & LS_{mki}(\mathbf{x})>0,\quad m=1,2,3,\quad k=3i+1,3i+2,3i+3;\\ & Q_i(\mathbf{x})>0;\qquad FO_{mli}(\mathbf{x})>0,\ m=1,2,3,\ l=1,\dots,q;\\ & U_{ir}(\mathbf{x})>0,\quad r=1,\dots,4;\\ & MO_{muij}(\mathbf{x})>0,\quad m,u=1,2,3;\\ & R_{ij}(\mathbf{x})>0,\quad i,j=0,\dots,n,\ j\neq i\},\end{aligned}$$

it is easily verified that the Lyapunov function candidate $L(\mathbf{x})$ satisfies the following properties:

(a) $L(\mathbf{x})$ is continuous and has first partial derivatives in the region $D(L)$ in the neighborhood of the point $\mathbf{x}_e$ of system (1);

(b) $L(\mathbf{x}_e) = 0$;

(c) $L(\mathbf{x}) > 0$ for all $\mathbf{x} \in D(L)/\mathbf{x}_e$;

(d) $\dot{L}(\mathbf{x}) \leq 0$ for all $\mathbf{x} \in D(L)$;

(e) $\dot{L}(\mathbf{x}_e) = 0$.

Hence, we can conclude that $L(\mathbf{x})$ is an appropriate Lyapunov function for system (1) that guarantees its stability:

Theorem 1. *The equilibrium point* $\mathbf{x}_e$ *of system* (1) *is stable provided the controllers* $(u_{i1}, u_{i2}, u_{i3}, u_{i4})$ *are as defined in* (15).

6. Implementation of the control laws. In this section, we demonstrate the effectiveness of the proposed motion planner by controlling the motion of a swarm of 2MMs in a fixed formation navigating in a constrained workspace. We verify numerically the stability and the convergence results obtained from the Lyapunov-based control scheme.

6.1. Scenario 1: 4-robot arrowhead formation. In this scenario we consider the motion of a 4-robot arrowhead formation. Basically we want the swarm of 2MMs to converge to a target position and attain the desired orientation, avoiding the obstacles in its path while maintaining an acceptable degree of formation stiffness. We have utilized the RK4 method to numerically integrate system (1). This enables us to obtain the solutions $(x_i, y_i, \theta_{i1}, \theta_{i2}, \theta_{i3}, v_i, \omega_{i1}, \omega_{i2}, \omega_{i3})$ and plot the points (x_i, y_i) in the z_1-z_2 plane until the points converge to a neighborhood of the target. The corresponding initial and final states, numerical values of the different parameters, workspace restrictions and other details are given in Table 1 and Table 2.

The nonlinear control laws were implemented to generate feasible maneuvers of the swarm in a fixed arrowhead formation. Figure 2 (a) shows the evolution of trajectories of the individual members of the swarm to the target configuration. Figure 2 (b) shows that the prescribed formation is maintained during the motion with slight

TABLE 1. Initial and final states.

	A_0	A_1	A_2	A_3
Rectangular Positions (x_i, y_i) (m)	$(7, 14)$	$(3, 17)$	$(3, 14)$	$(3, 11)$
Angular Positions $(\theta_{i1}, \theta_{i2}, \theta_{i3})$ (rad)	$(0, \frac{\pi}{3}, -\frac{2\pi}{3})$	$(0, \frac{\pi}{3}, -\frac{2\pi}{3})$	$(0, \frac{\pi}{3}, -\frac{2\pi}{3})$	$(0, \frac{\pi}{3}, -\frac{2\pi}{3})$
Translational velocities (m/s)	$v_0 = 3$	$v_1 = 3$	$v_2 = 3$	$v_3 = 3$
Rotational Vel. $(\omega_{i1}, \omega_{i2}, \omega_{i3})$ (rad/s)	$(0.3, 0.1, 0.1)$	$(0.3, 0.1, 0.1)$	$(0.3, 0.1, 0.1)$	$(0.3, 0.1, 0.1)$
Target Centers (p_{i1}, p_{i2}) (m)	$(27, 14)$	$(23, 17)$	$(23, 14)$	$(23, 11)$
Final Orientations (p_{i3}, p_{i4}, p_{i5}) (rad)	$(0, \frac{\pi}{4}, -\frac{\pi}{2})$	$(0, \frac{\pi}{4}, -\frac{\pi}{2})$	$(0, \frac{\pi}{4}, -\frac{\pi}{2})$	$(0, \frac{\pi}{4}, -\frac{\pi}{2})$

TABLE 2. Values of constraints and parameters.

Clearance Parameters	$\varepsilon_1 = 0.2m$, $\varepsilon_2 = 0.1m$, $\varepsilon_3 = 0.3m$
Robot Dimensions	$\ell_0 = 1.2\ m$, $b_0 = 0.7\ m$, $\ell_1 = \ell_2 = 0.8\ m$
Ghost Target Parameters	$(k_{11}, k_{12}) = (2.5\ m, -3\ m)$; $(k_{21}, k_{22}) = (2.5\ m, 0\ m)$; $(k_{31}, k_{32}) = (2.5\ m, 3\ m)$
Obstacle Center, Radius	$(o_{11}, o_{12}) = (11\ m, 17\ m)$, $ro_1 = 2\ m$
Max. distance (M_{ij})	$M_{01} = 5.5\ m$; $M_{02} = 4.5\ m$, $M_{03} = 4.5\ m$; $M_{10} = 5.5\ m$, $M_{12} = 3.5\ m$, $M_{13} = 6.5\ m$; $M_{20} = 4.5\ m$, $M_{21} = 3.5\ m$, $M_{23} = 4.5\ m$; $M_{30} = 5.5\ m$;$M_{31} = 6.5\ m$, $M_{32} = 4.5\ m$
Heading	$\varepsilon_{0i} = 0.2\ rad$, for $i = 1, 2, 3$
Angle Gain Parameters	$\rho_{i1} = \rho_{i2} = \rho_{i3} = 1$, for $i = 0, 1, 2, 3$
Max. Steering Angle	$\phi_{\max} = 7\pi/18\ rad$
Max. Velocities	$v_{\max} = 10\ m/s$; $\omega_{2\max} = \omega_{3\max} = 1\ rad/s$
Top, Right Boundaries	$\eta_1 = \eta_2 = 28\ m$
Control Parameters	$\alpha_{is} = 0.01$, $s = 1, \ldots, 8$; $\gamma_{im1} = 0.5$, $m = 1, 2, 3$; $\zeta_{imk} = 1.2$; $\xi_{ip} = 0.5$, $p = 1, 2, 3$; $\beta_{ir} = 0.1$, $r = 1, \ldots, 4$; $\psi_{ij} = 0.01$; $\varphi_{muij} = 0.5$, $m, u = 1, 2, 3$,$i, j = 0, \ldots, 3$, $j \neq i$; $\sigma_1 = \sigma_2 = \sigma_3 = 0.1$
Convergence Parameters	$\delta_{i1} = \delta_{i2} = \delta_{i3} = \delta_{i4} = 15$ for $i = 0, 1, 2, 3$

distortions to the constellation when the swarm avoids the fixed obstacle in its path. However, the prescribed low-degree formation is re-established before the convergence of the swarm to its target configuration.

We have also generated the graph of orientations of the different bodies of the leader-robot (see Figure 2 (c)). It can clearly be seen that the desired final orientation of each body of the 2-link mobile manipulator is achieved at the target; proving the effectiveness of the MDT. Figure 2 (d) shows the evolution of the orientations of the end-effectors of the leader and the follower robots. This also proves the low-degree formation of the swarm and the effectiveness of the obstacle avoidance function governing its heading. Finally, Figures 2 (e) and 2 (f) show the behavior of the nonlinear controllers for the leader-robot. Convergence at the target configuration is observed in both figures, which clearly validate the effectiveness of the proposed controllers. Similar trends were observed with the follower-robots.

6.2. Scenario 2: 5-robot X-Shaped formation. In this scenario, we have considered the leader-robot at the center of an X-shaped formation with a follower-robot positioned at each vertex. The formation has to maneuver from an initial to a final state, whilst avoiding all fixed and moving obstacles in its path. Tables 3 and 4 provide values for the initial conditions, constraints and the different parameters utilized in this simulation, however, only those that are different from Scenario 1. The control laws were implemented to generate feasible trajectories.

Figure 3 (a) shows the trajectories of the individual 2MM of the swarm fixed in a X-shaped formation. Figure 3 (b) shows that the prescribed formation is maintained during the motion. It is also clear from the figure that there is a temporary distortion of the constellation when the swarm gets closer to the fixed obstacle, but the original formation is re-established soon after the well-choreographed collision avoidance. The controllers also guarantee re-establishment of the predefined formation when a 2MM is getting closer or lagging behind another 2MM. The behaviors of the non-linear controllers of the leader-robot are shown in Figures 4 and 5, indicating its convergent nature.

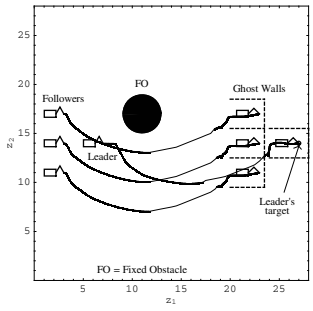

(a) Integrated trajectories.

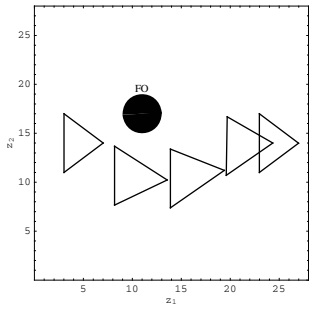

(b) Arrowhead formation.

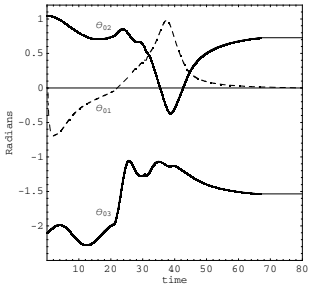

(c) Orientations of the wheeled platform (θ_{01}), link 1 (θ_{02}) and link 2 (θ_{03}) of A_0.

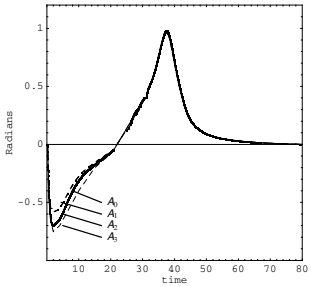

(d) Orientations: End-Effectors of the robots in formation.

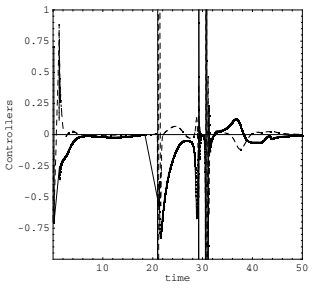

(e) The translational, u_{01} (solid line) and rotational u_{02} acceleration of the wheeled platform of A_0.

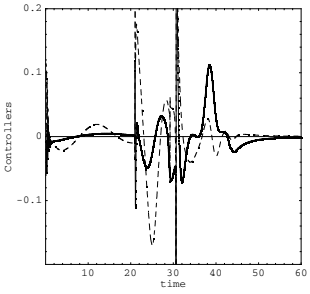

(f) The rotational accelerations, u_{03} (solid line) and u_{04} of link 1 and link 2 of A_0.

FIGURE 2. The evolution of state variables and the swarm formation for Scenario 1.

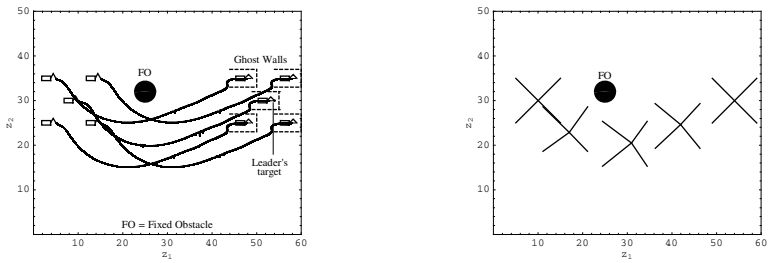

(a) Integrated trajectories (b) X-shaped formation

FIGURE 3. The evolution of trajectories and the prescribed formation for Scenario 2.

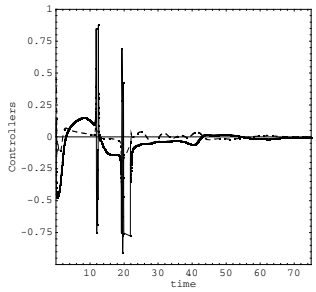

FIGURE 4. The translational, u_{01} (solid line) and rotational u_{02} acceleration of the platform.

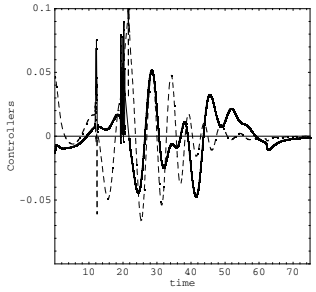

FIGURE 5. The rotational accelerations, u_{03} (solid line) and u_{04} of the link 1 and link 2.

TABLE 3. Initial and final configurations.

A_0	A_1	A_2	A_3	A_4	
Rect. Positions (x_i, y_i)	$(10, 30)$	$(15, 35)$	$(15, 25)$	$(5, 25)$	$(5, 35)$
Angular Positions $(\theta_{i1}, \theta_{i2}, \theta_{i3})$	$(0, \frac{\pi}{3}, -\frac{2\pi}{3})$	$(0, \frac{\pi}{3}, -\frac{2\pi}{3})$	$(0, \frac{\pi}{3}, -\frac{2\pi}{3})$	$(0, \frac{\pi}{3}, -\frac{2\pi}{3})$	$(0, \frac{\pi}{3}, -\frac{2\pi}{3})$
Translational velocities	$v_0 = 2$	$v_1 = 2$	$v_2 = 2$	$v_3 = 2$	$v_4 = 2$
Rotational Vel. $(\omega_{i1}, \omega_{i2}, \omega_{i3})$	$(0.3, 0.1, 0.1)$	$(0.3, 0.1, 0.1)$	$(0.3, 0.1, 0.1)$	$(0.3, 0.1, 0.1)$	$(0.3, 0.1, 0.1)$
Target Centers (p_{i1}, p_{i2})	$(54, 30)$	$(59, 35)$	$(59, 25)$	$(49, 25)$	$(49, 35)$
Final Orientations (p_{i3}, p_{i4}, p_{i5})	$(0, \frac{\pi}{4}, -\frac{\pi}{2})$	$(0, \frac{\pi}{4}, -\frac{\pi}{2})$	$(0, \frac{\pi}{4}, -\frac{\pi}{2})$	$(0, \frac{\pi}{4}, -\frac{\pi}{2})$	$(0, \frac{\pi}{4}, -\frac{\pi}{2})$

TABLE 4. Values of constraints and parameters.

Robot Dimensions	$\ell_0 = 2.0\ m$, $b_0 = 1.0\ m$, $\ell_1 = \ell_2 = 1.2\ m$
Ghost Target Parameters	$(k_{11}, k_{12}) = (-7.5\ m, -5\ m)$, $(k_{21}, k_{22}) = (-7.5\ m, 5\ m)$; $(k_{31}, k_{32}) = (1.5\ m, 5\ m)$, $(k_{41}, k_{42}) = (1.5\ m, -5\ m)$
Obstacle Center, Radius	$(o_{11}, o_{12}) = (25\ m, 32\ m)$, $ro_1 = 2.5\ m$
Max. distance (M_{ij})	$M_{01} = 8.0\ m$; $M_{02} = 8.0\ m$, $M_{03} = 8.0\ m$, $M_{04} = 8.0\ m$; $M_{10} = 8.0\ m$, $M_{12} = 11.0\ m$, $M_{13} = 15.0\ m$, $M_{14} = 11.0\ m$; $M_{20} = 8.0\ m$, $M_{21} = 11.0\ m$, $M_{23} = 11.0\ m$, $M_{24} = 15.0\ m$; $M_{30} = 8.0\ m$, $M_{31} = 15.0\ m$, $M_{32} = 11.0\ m$, $M_{34} = 11.0\ m$; $M_{40} = 8.0\ m$, $M_{41} = 11.0\ m$, $M_{42} = 15.0\ m$, $M_{43} = 11.0\ m$
Top, Right Boundaries	$\eta_1 = 60\ m$; $\eta_2 = 50\ m$
Control Parameters	$\alpha_{is} = 0.01$, $s = 1, \ldots, 8$; $\gamma_{im1} = 0.5$, $m = 1, 2, 3$; $\zeta_{imk} = 1.2$; $\xi_{ip} = 0.5$, $p = 1, 2, 3$; $\beta_{ir} = 0.1$, $r = 1, \ldots, 4$; $\psi_{ij} = 0.01$; $\varphi_{muij} = 0.5$, $m, u = 1, 2, 3$,$i, j = 0, \ldots, 4$, $j \neq i$; $\sigma_1 = \sigma_2 = \sigma_3 = 0.1$
Convergence Parameters	$\delta_{i1} = \delta_{i2} = \delta_{i3} = \delta_{i4} = 15$ for $i = 0, \ldots, 4$

7. Concluding remarks. We have presented a set of continuous time-invariant acceleration control laws that successfully tackles the problem of formation control of a swarm of 2-link mobile manipulators in *a priori* known environment. The advancement of the prescribed formation was via the moving ghost targets, a variant of the leader-follower scheme. Synthesis of the controllers for the swarm was for the first time attempted via the Lyapunov-based control scheme, which inherently guaranteed stability of the kinodynamic system. The control scheme successfully encompasses changes to the swarm heading and can easily be modified to address scalability of the formations.

The tuning parameters from the control scheme provide an added degree of control of the subtasks and also ensured maintenance of

the prescribed formation. A new algorithm was integrated to the Lyapunov-based control scheme to establish and maintain prescribed formations, but allowing slight distortions in order to avoid obstacles directly in the path of the procession. After avoidance the swarm was forced back into constellation where the original formation was re-established. For the first time, final orientations of the swarm in a fixed formation was addressed via the use of MDT and ghost walls. The simulation results confirm the performance of the controller and validate the stability and convergence of the swarm of 2MMs.

In summary, our decentralized continuous control laws derived from the Lyapunov-based control scheme demonstrated autonomy and to a certain extent, the multitasking capabilities of homogeneous multi-agents seen in nature. A sequel of this paper will utilize the Lyapunov-based control scheme to address formation control of swarms in dynamic topologies.

REFERENCES

1. L. Barnes, W. Alvis, M. Fields, K. Valavanis and W. Moreno, *Heterogeneous swarm formation control using bivariate normal functions to generate potential fields*, Proc. IEEE Workdshop on Distributed Intelligent Systems: *Collective intelligence and its application*, Vol. 4, Prague, June 2006.

2. R.W. Brockett, *Differential geometry control theory*, in *Asymptotic stability and feedback stabilisation*, Springer-Verlag, New York, 1983.

3. U. Chand, *Control of cooperating car-like multi-agents in constrained environments*, Master's thesis, University of the South Pacific, 2007.

4. D.E. Chang, S.C. Shadden, J.E. Marsden and R. Olfati-Saber, *Collision avoidance for multiple agent systems*, Proc. 42nd IEEE Conf. Decision and Control, Maui, Hawaii, December 2003.

5. D. Crombie, *The examination and exploration of algorithms and complex behavior to realistically control multiple mobile robots*, Master's thesis, Australian National University, 1997.

6. G.H. Elkaim and R.J. Kelbley, *A lightweight formation control methodology for a swarm of non-holonomic vehicles*, in IEEE Aerospace Conference, 2006.

7. T. Ikeda, J. Jongusuk, T. Ikeda, and T. Mita, *Formation control of multiple nonholonomic mobile robots*, Electrical Engineering in Japan **157** (2006), 81–88.

8. W. Kang, N. Xi, J. Tan and Y. Wang, *Formation control of multiple autonomous robots*: *Theory and experimentation*, Intelligent Automation Soft Computing **10** (2004), 1–17.

9. O. Khatib, *Real time obstacle avoidance for manipulators and mobile robots*, Inter. J. Robotics Research **7** (1986), 90–98.

10. I. Kolmanovsky and N. McClamroch, *Developments in nonholonomic control problems*, IEEE Control Systems Magazine **15** (1995), 20–36.

11. J-C. Latombe, *Potential field method*, in *Robot motion planning*, Kluwer Academic Publishers, Boston, 1991.

12. L.-F. Lee, R. Bhatt and V. Krovi, *Comparison of alternate methods for distributed motion planning of robot collectives within a potential field framework*, in Proc. IEEE Internat. Conf. Robotics Automation, April 2005, 99–104.

13. L.-F. Lee and V. Krovi, *A standardized testing-ground for artificial potential-field based motion planning for robot collectives*, in Proc. Performance Metrics for Intelligent Systems Workshop, Gaithersburg, August 2006.

14. X. Li and J. Xiao, *A biologically inspired controller for swarms in dynamcia environments*, Internat. J. Intelligent Control Systems **11** (2006), 154–162.

15. Y. Liang and H-H. Lee, *Decentralized formation control and obstacle avoidance for multiple robots with nonholonomic constraints*, in Proc. Amer. Control Conf., Minneapolis, MN, June 2006, 5596–5601.

16. M. Lindhé, *A flocking and obstacle avoidance algorithm for mobile robots*, Master's thesis, KTH School of Electrical Engineering, Stockholm, Sweden, June 2004.

17. P. Ögren, *Formations and obstacle avoidance in mobile robot control*, Master's thesis, Royal Inst. Technology, Stockholm, Sweden, June 2003.

18. C.W. Reynolds, *Flocks, herds, and schools: A distributed behavioral model, in computer graphics*, in Proc. 14th Annual Conf. on Computer Graphics and Interactive Techniques, New York, 1987, 25–34.

19. E. Rimon, *Exact robot navigation using artificial potential functions*, IEEE Trans. Robotics Automation **8** (1992), 501–517.

20. F.E. Schneider and D. Wildermuth, *Posture control and stability of a general 1-trailer system: A Lyapunov approach*, in Internat. Conf. on Robotics, Intelligent Systems and Signal Processing, Changsha, China, October 2003.

21. B. Sharma, *New directions in the applications of the Lyapunov-based control scheme to the findpath problem*, Ph.D. dissertation, July 2008.

22. B. Sharma and J. Vanualailai, *Lyapunov stability of a nonholonomic car-like robotic system*, Nonlinear Stud. **14** (2007), 143–160.

23. B. Sharma, J. Vanualailai and A. Chandra, *Dynamic trajectory planning of a standard trailer system*, Far East J. Appl. Math. **28** (2007), 465–486.

24. B. Sharma, J. Vanualailai and S. Nakagiri, *Posture control and stability of a general 1-trailer system: A Lyapunov approach*, in RIMS Symposium, Kyoto University, Japan, November 2006, 134–143.

25. B. Sharma, J. Vanualailai and A. Prasad, *A Lyapunov-based path planning and obstacle avoidance of a two-link manipulator on a wheeled platform*, Internat. J. Information Tech. **14** (2008), 57–75.

26. B. Sharma, J. Vanualailai, K. Raghuwaiya and A. Prasad, *New potential field functions for motion planning and posture control of 1-trailer systems*, Internat. J. Math. Computer Sci. **3** (2008), 45–71.

27. H. Tanner, A. Jadbabaie and G.J. Pappas, *Stable flocking of mobile agents*, Part I: *Fixed topology*, in Proc. 42nd IEEE Conf. Decision and Control, 2003, 2010–2015.

28. J. Vanualailai, J. Ha and S. Nakagiri, *A collision and attraction problem for a vehicle*, in RIMS Symposium, Kyoto University, Japan, November 2003.

29. J. Vanualailai, B. Sharma and A. Ali, *Lyapunov-based kinematic path planning for a 3-link planar robot arm in a structured environment*, Global J. Pure Appl. Math. **3** (2007), 175–190.

School of Computing, Information & Mathematical Sciences, University of the South Pacific, Suva, Fiji
Email address: sharma_b@usp.ac.fj

School of Computing, Information & Mathematical Sciences, University of the South Pacific, Suva, Fiji
Email address: vanualailai@usp.ac.fj

School of Computing, Information & Mathematical Sciences, University of the South Pacific, Suva, Fiji
Email address: avinesh.prasad@usp.ac.fj